High Segmentation, Radiation-Hard Calorimetry Options for FCC

Y. Onel[1], B. Bilki[1,2,3]

[1] University of Iowa, Iowa City, USA

[2] Beykent University, Istanbul, Turkey

[3] Turkish Accelerator and Radiation Laboratory, Ankara, Turkey

Second Annual U.S. Future Circular Collider (FCC) Workshop 2024

25 - 27 Mar, 2024

Trend in Calorimetry

Tower geometry

Energy is integrated over large volumes into single channels

Readout typically with high resolution

Individual particles in a hadronic jet not resolved

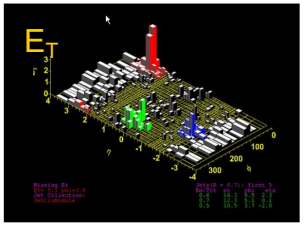

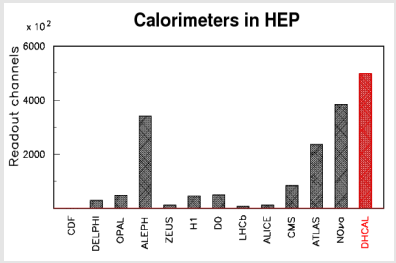

Imaging calorimetry

Large number of calorimeter readout channels (~10^7)

Option to minimize resolution on individual channels

Particles in a jet are measured individually

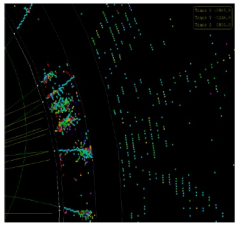

Particle Flow Algorithms (PFAs)

Attempt to measure the energy/momentum of each particle with the detector subsystem providing the best resolution

Maximum exploitation of precise tracking measurement

- Large radius and length to separate the particles
- Large magnetic field for high precision momentum measurement
- “no” material in front of calorimeters (stay inside coil)
- Small Moliere radius of calorimeters to minimize shower overlap
- High granularity of calorimeters to separate overlapping showers

Emphasis on tracking capabilities of calorimeters

Digital Hadron Calorimetry

Development of the Digital Hadron Calorimeter

- Develop a tracking Hadron Calorimeter
- Implement digital readout (1-bit) to maximize the number of readout channels
- Place the front-end electronics in the detector

The active medium should:

- Be planar and scalable to large sizes
- Not necessarily be proportional (only yes/no for the traversing particle)
- Be easy to construct, robust, reliable, easy to operate, …

→ Resistive Plate Chambers

Resistive Plate Chambers (RPCs)

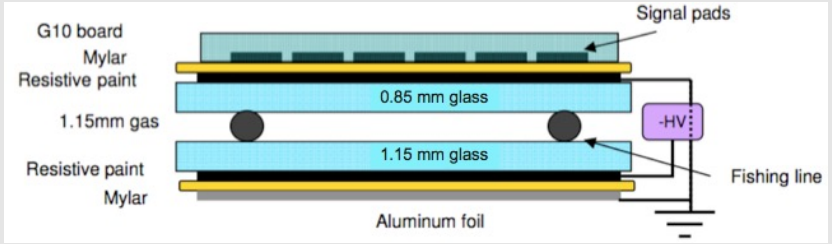

Gas: Tetrafluorethane (R134A) : Isobutane : Sulfurhexafluoride (SF_6) with the following ratios 94.5 : 5.0 : 0.5

High Voltage: 6.3 kV (nominal)

Average efficiency: 96 %

Average pad multiplicity: 1.6

The DHCAL Prototype

Description

Hadronic sampling calorimeter

Designed for future electron-positron collider (ILC)

54 active layers (~1 m^2)

Resistive Plate Chambers with 1 x 1 cm^2 pads

→ ~500,000 readout channels

Electronic readout

1 – bit (digital)

Tests at FNAL

with Iron absorber in 2010 – 2011

with no absorber in 2011

Tests at CERN

with Tungsten absorber in 2012

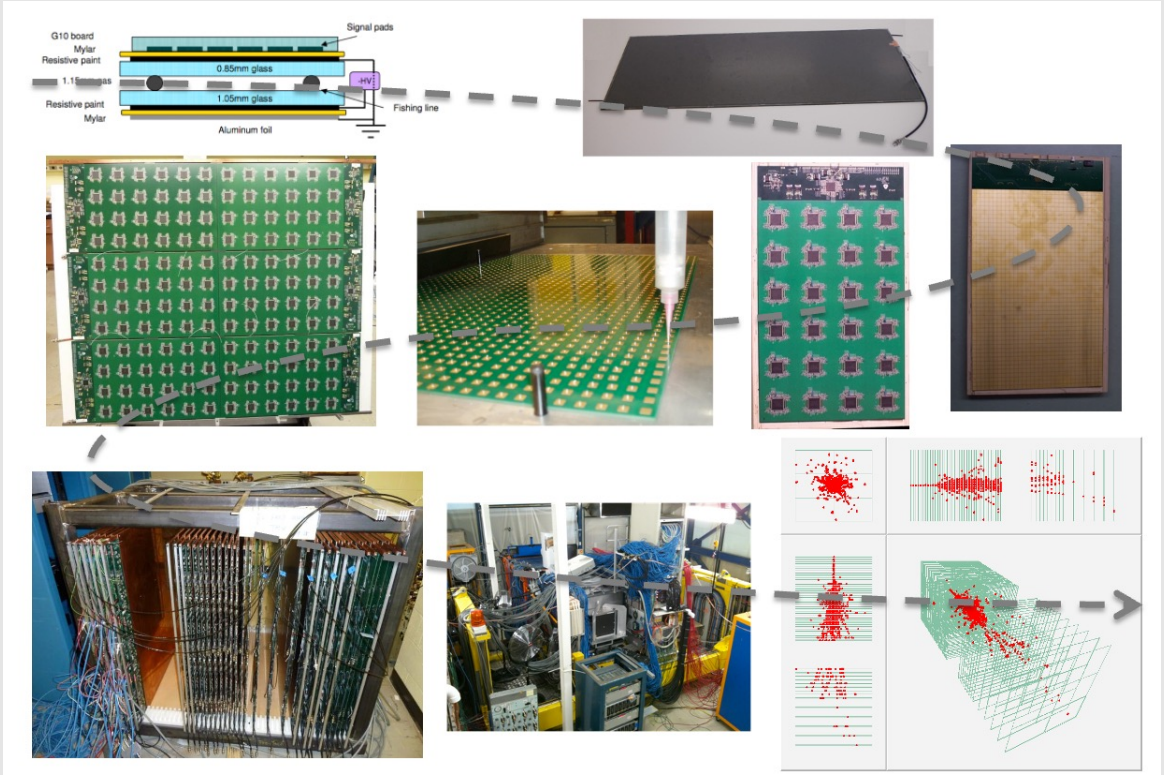

Readout Electronics Overview

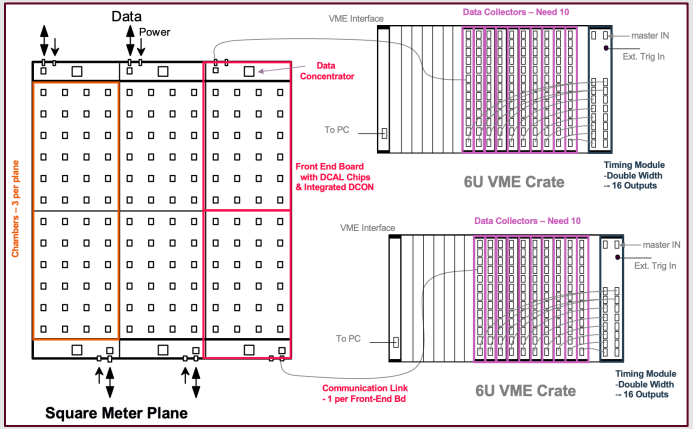

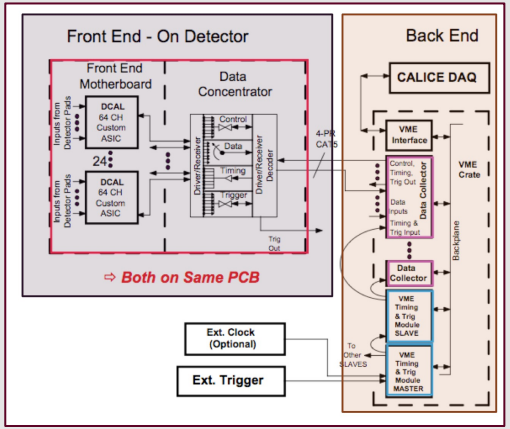

The DCAL Chip

Developed by

FNAL and Argonne

Input

64 channels
High gain (GEMs, micromegas…) with minimum threshold ~ 5 fC
Low gain (RPCs) with minimum threshold ~ 30 fC

Threshold

Set by 8 – bit DAC (up to ~600 fC)
Common to 64 channels

Readout

Triggerless (noise measurements)
Triggered (cosmic, test beam)

Versions

DCAL I: initial round (analog circuitry not optimized)
DCAL II: some minor problems (used in vertical slice test)
DCAL III: no identified problems (final production)

Production of DCAL III

11 wafers, 10,300 chips, fabricated, packaged, tested

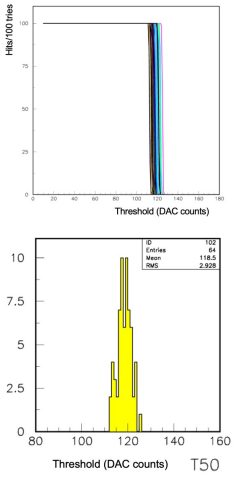

Front-end Electronics and Gluing

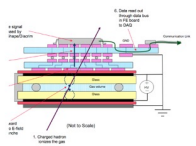

Front-end board (FEB) assembly

- Build electronics and pad boards separately to avoid blind and buried vias
- Each FEB contains 1536 channels
- A data concentrator is implemented
- Test electronics (noise rates, threshold curves,…)

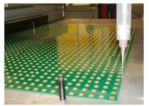

Glue Robot

- Glue is a conductive epoxy
- Robot precisely places glue dots
- 0.001" thick plastic film used as spacers
- dried in oven over night
- 10 boards/day
- >300 FEB fabricated

Cassette Assembly

- Cassette is compressed horizontally with a set of 4 (Badminton) strings
  - Strings are tensioned to ~20 lbs each
  - ~45 minutes/cassette

Fe-DHCAL at Fermilab

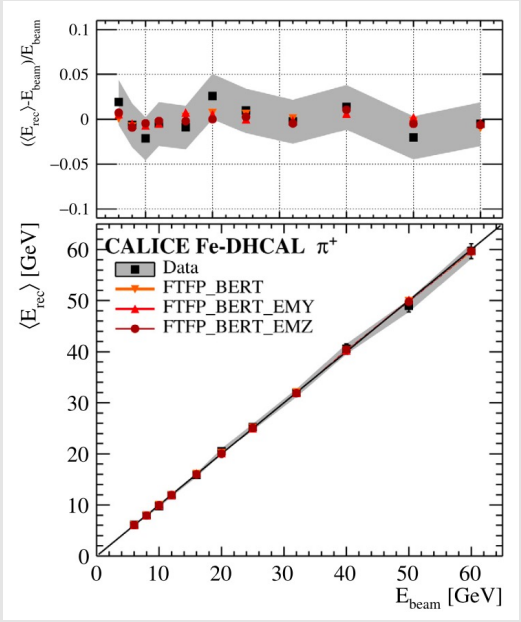

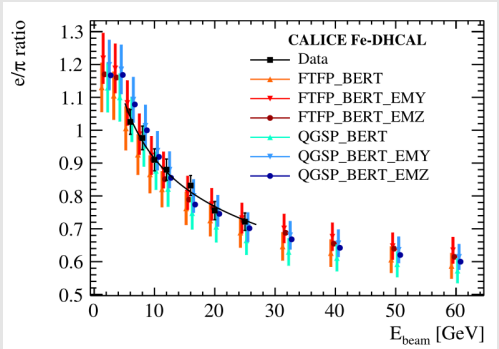

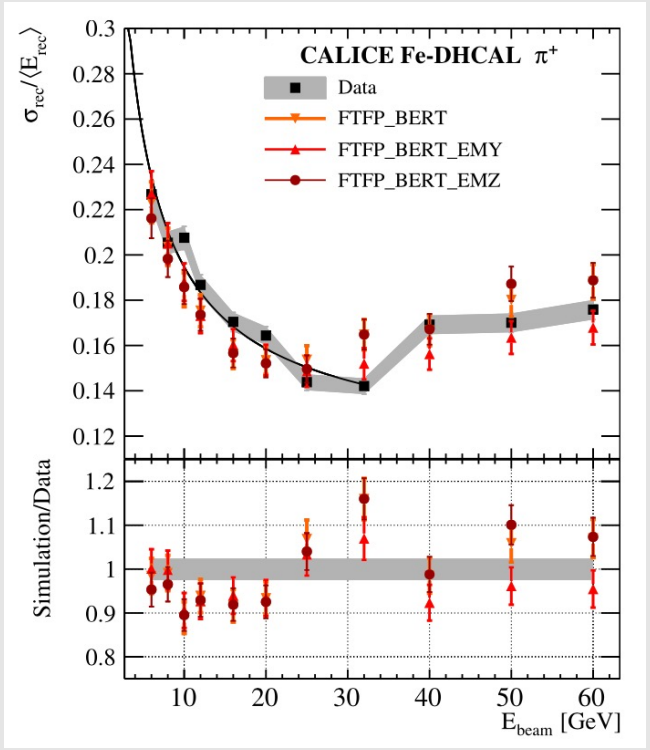

$$\frac{\sigma}{E} = \frac{(51.5 \pm 1.5)\%}{\sqrt{E}} \oplus (10.6 \pm 0.5)\%$$

M. Chefdeville, et.al., Nucl. Instr. And Meth. A 939, 89, 2019

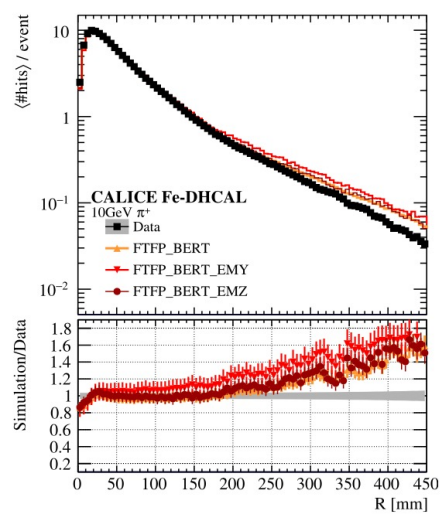

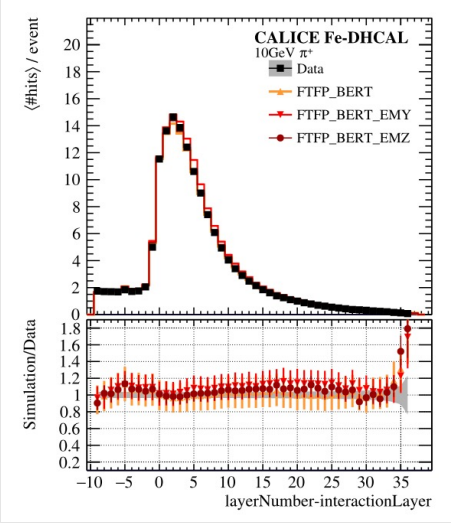

W-DHCAL at CERN – Combined PS and SPS Measurements

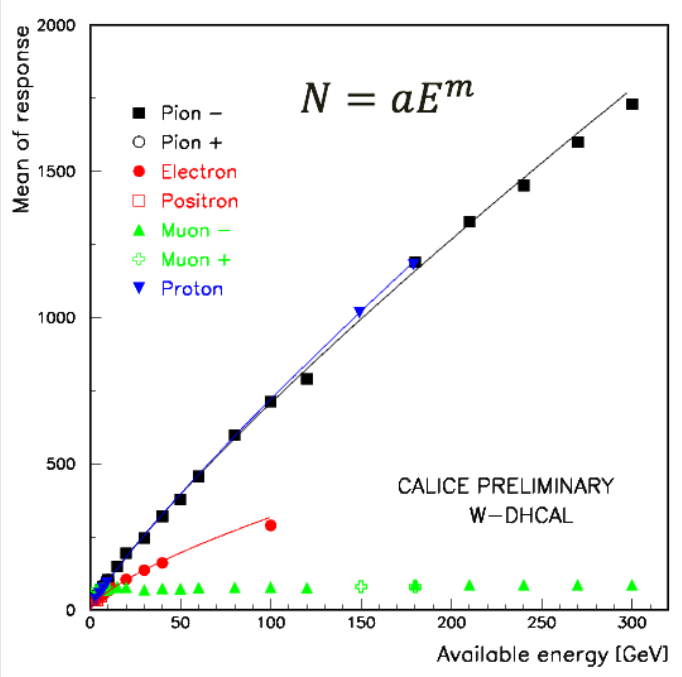

Particle	a	m
Pions	14.7	0.84
Protons	13.6	0.86
Electrons	12.7	0.70

W-DHCAL with 1 x 1 cm^2

Highly over-compensating compared to the Fe-DHCAL for the entire energy range.

Particle	α	c
Pions	(68.0±0.4)%	(5.4±0.7)%
Electrons	(29.4±0.3)%	(16.6±0.3)%

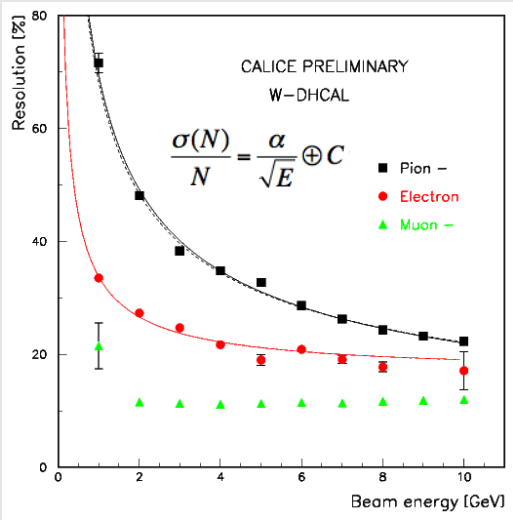

Simulation of the DHCAL Response

- is particularly challenging
- shows significant improvements in newer versions of Geant4 and EM physics packages
- Involves several interconnected steps:

1. The primary ionization locations in the gas gaps of the RPCs are obtained from Geant4.

2. The ionization charges are sampled from the distribution obtained with the analog readout of a DHCAL RPC.

3. A dedicated software called RPCSim was developed to distribute the generated charge over the pads, apply the threshold and reconstruct the hits.

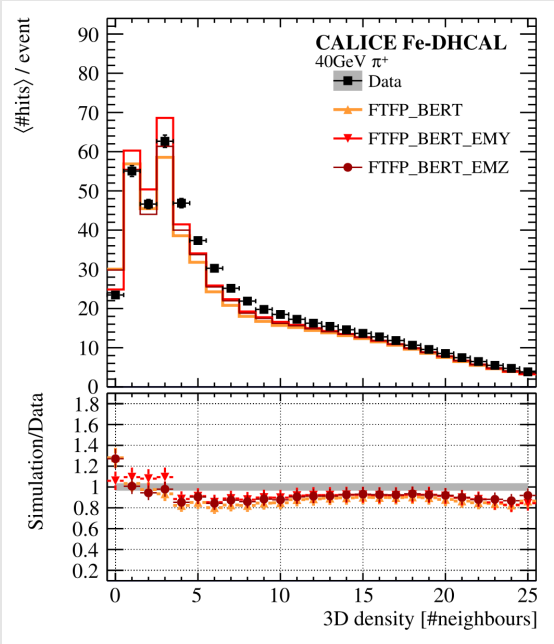

3D density of hits for 40 GeV π^+ showers in the DHCAL with iron absorbers (Fe-DHCAL)

The disagreements are at the very fine level of detail which is not available in conventional calorimeters. ➔ Work ongoing.

Recent Hardware Developments
For
Digital Hadron Calorimetry

1-glass RPCs

Offers many advantages

Pad multiplicity close to one
→ easier to calibrate
Better position resolution
→ if smaller pads are desired
Thinner
→ $t = t_{chamber} + t_{readout} = 2.4 + \sim 1.5$ mm
→ saves on cost
Higher rate capability
→ roughly a factor of 2

Status

Built several large chambers
Tests with cosmic rays very successful
→ chambers ran for months without problems
Both efficiency and pad multiplicity look good
Good performance in the test beam

B. Bilki, et.al., JINST 5, P05003, 2015

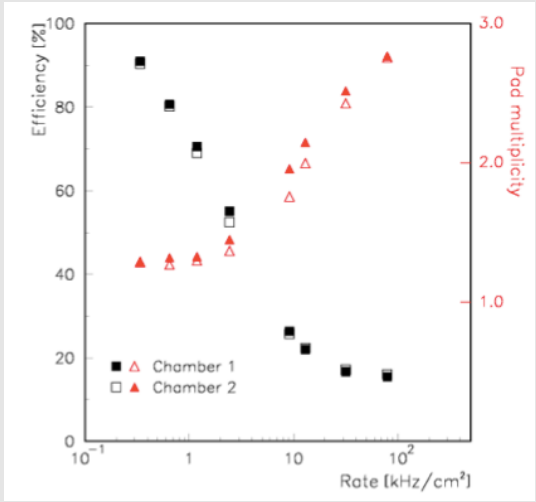

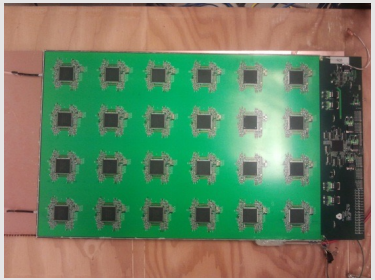

Efficiency

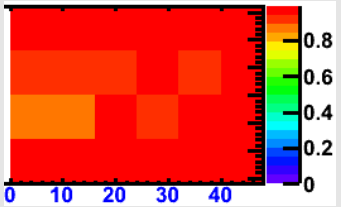

Pad multiplicity

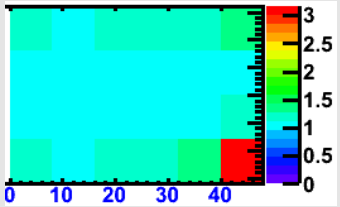

Development of Hybrid RPCs

Probing a hybrid readout where part of the electron multiplication is transferred to a thin film of high secondary emission yield material coated on the readout pad with the purpose of reducing/removing gas flow and enabling the utilization of alternative gases.

Built several 10 cm x 10 cm chambers with single pad readout.

Coating of Al_2O_3 made with magnetron sputtering.

Coating of TiO_2 made with airbrushing after dissolving TiO_2 in ethanol.

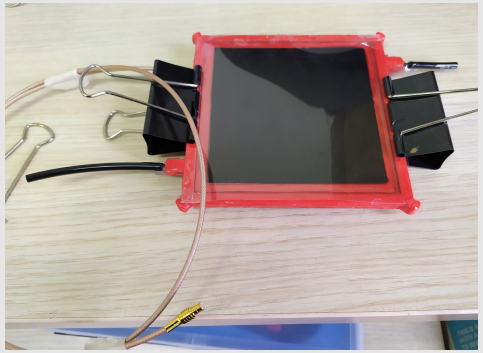

Cosmic muon response

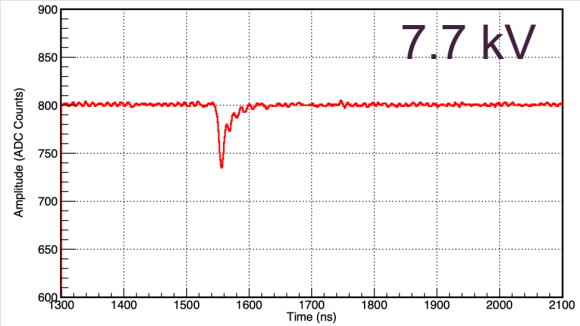

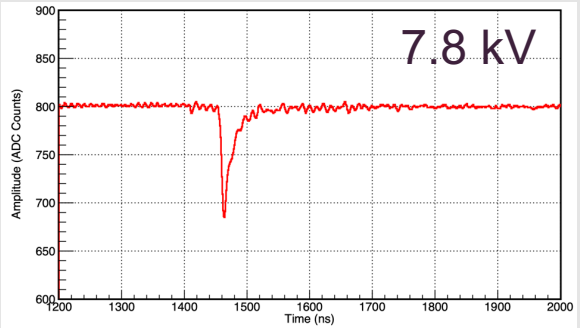

Tests of First-Generation Hybrid RPCs

We tested the first-generation hybrid RPCs as well as the standard 1-glass and 2-glass RPCs at Fermilab test beam. The lateral size of the chambers was 10 cm x 10 cm, the gas gap was 1.3 mm and the gas mixture was the DHCAL RPC gas mixture R134A : Isobutane : SF_6 ; 94.5 : 5.0 : 0.5 at 2-3 cc/min flow rate (lower than the nominal 5 cc/min).

Chambers tested and their 90% efficiency crossing HV:

1. 2-glass RPC (8.5 kV)
2. 1-glass RPC (7.5 kV)
3. 500 nm Al_2O_3 (v1) (6.5 kV)
4. 350 nm Al_2O_3 (v2) (6.5 kV)
5. 1 mg/cm^2 TiO_2 (v1) (6.5 kV)
6. 0.5 mg/cm^2 TiO_2 (v2) (6.5 kV)
7. 0.15 mg/cm^2 TiO_2 (v3) (7.5 kV)

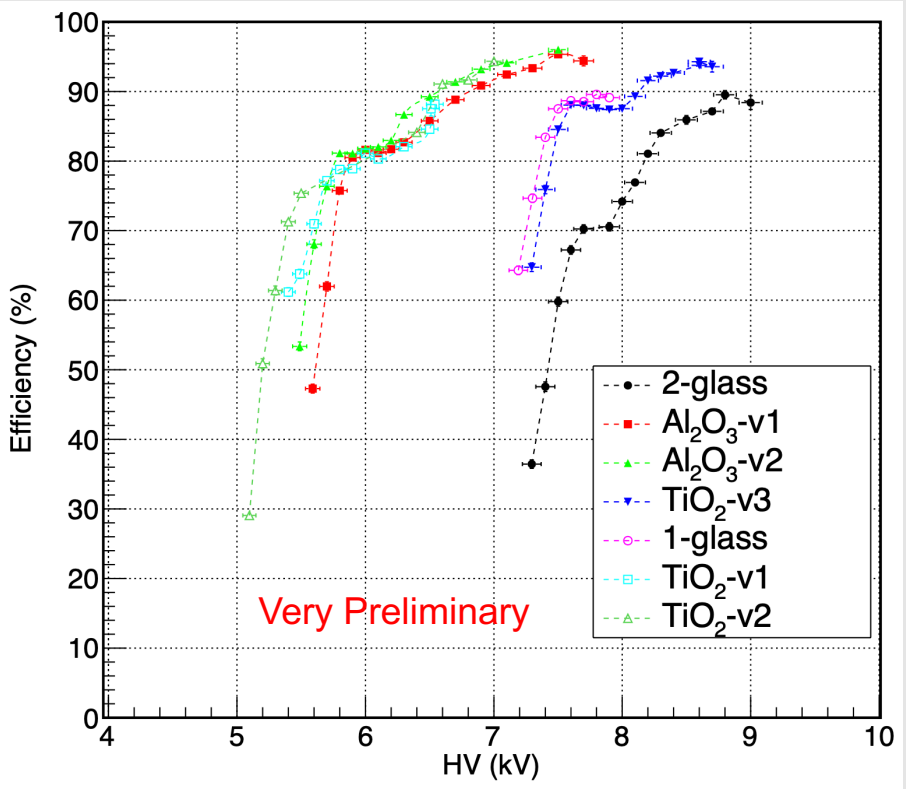

The charge multiplication in the secondary emission layer is qualitatively validated.

Efficient if charge > 300 fC

Rate capability of RPCs

Measurements of efficiency

With 120 GeV protons
In Fermilab test beam

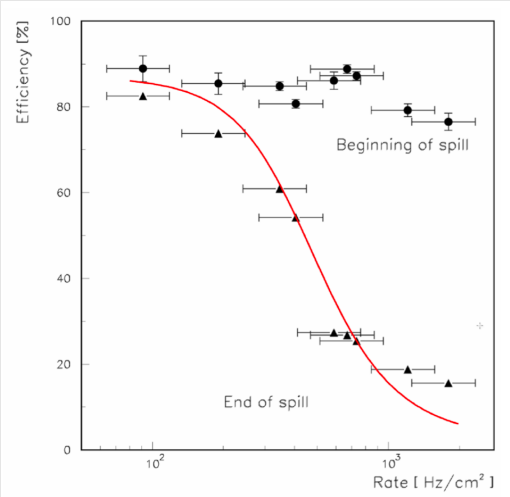

Rate limitation

NOT a dead time
But a loss of efficiency

Theoretical curves

Excellent description of effect

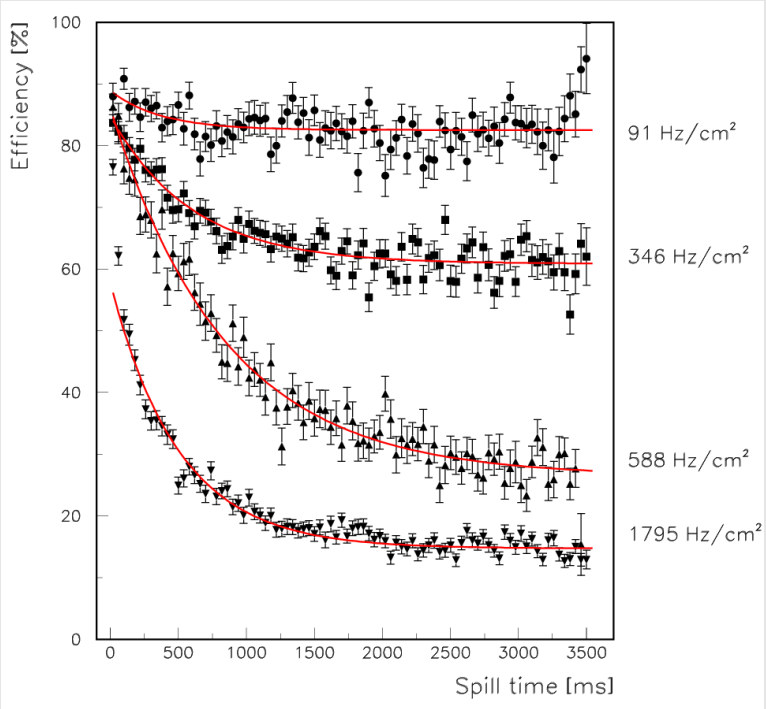

Rate capability depends on

The bulk resistivity R_{bulk} of the resistive plates

Lower bulk resistivity → higher rate capability

B.Bilki et al., JINST 4 P06003, 2009

Development of semi-conductive glass

Co-operation with **COE college** (Iowa)

Vanadium based glass

Resistivity tunable

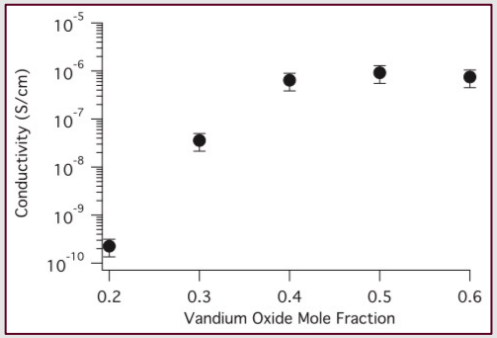

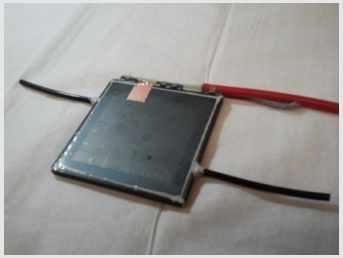

SLS: Soda lime silicate
ZTV: Zinc tellurium vanadate

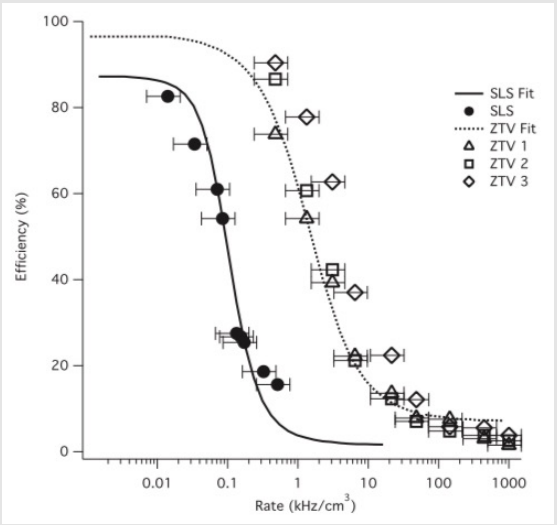

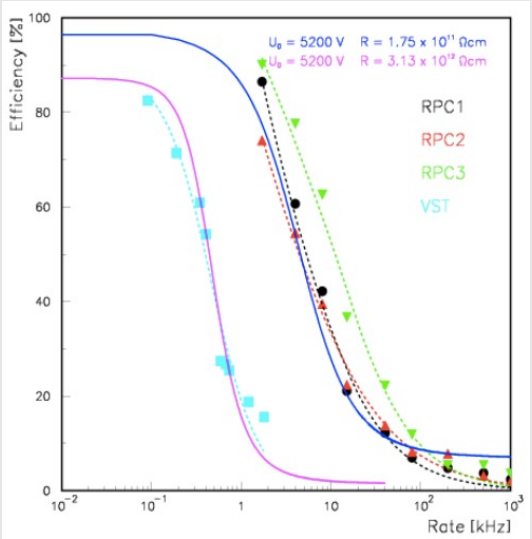

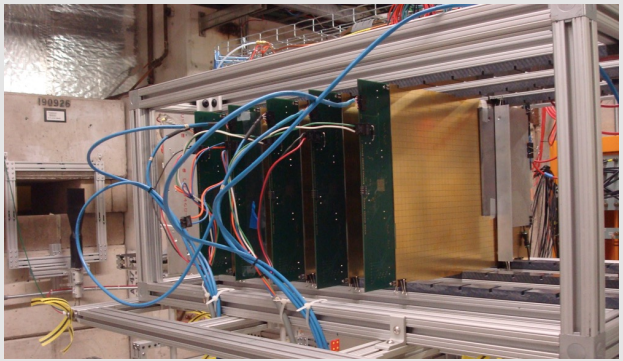

N. Johnson et al., Int. J. Appl. Glass Sci. 6, 26, 2015

Further Development of High-Rate RPCs

RPC design	Number of glass plates	Area A [cm^2]	Bulk resistivity ρ [Ωcm]	Total thickness t of the glass [cm]	Conductance per area of the glass $G = (\rho \cdot t)^{-1}$ [Ω^{-1}cm^{-2}]	Rate at 50% efficiency [Hz/cm^2]	
1	2	400	4.7×10^{12}	0.22	1.0×10^{-12}	300	Soda-lime
2	1	1536	3.7×10^{12}	0.11	2.4×10^{-12}	1500	Soda-lime
3	2	400	6.3×10^{10}	0.28	5.6×10^{-11}	15,000	Schott

M. Affatigato et al., JINST 10 P10037, 2015

1. *2-glass RPCs with standard glass*
   The chambers were built with two standard soda-lime float glass plates with a thickness of 1.1 mm each. The gas gap was 1.2 mm. The chambers were 20 x 20 cm^2 in size.

2. *1-glass RPCs with standard glass*
   The chambers were built with one standard soda-lime float glass plate with a thickness of 1.15 mm. The gas gap was also 1.15 mm. The size of the chamber was dictated by the size of the readout board, i.e. 32 x 48 cm^2. With only one glass plate the gas volume is defined by the glass plate and the anode board. Thus, the readout pads are located directly in the gas volume.

3. *2-glass RPCs with semi-conductive glass*
   These chambers utilize semi-conductive glass with a bulk resistivity several orders of magnitude smaller than standard soda-lime float glass. The glass, *model S8900*, is available from Schott Glass Technologies Inc. The gas gap of these chambers was also 1.15 mm and the area of the chambers measured 20 x 20 cm^2. With 1.4 mm thickness, the glass plates were somewhat thicker than for the other designs.

Further Development of High-Rate RPCs

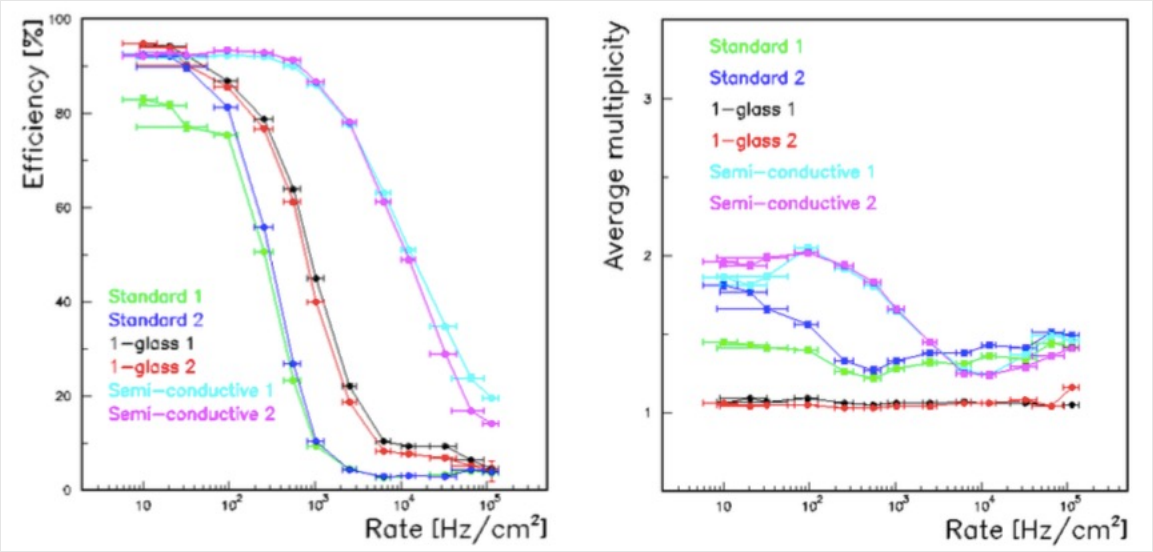

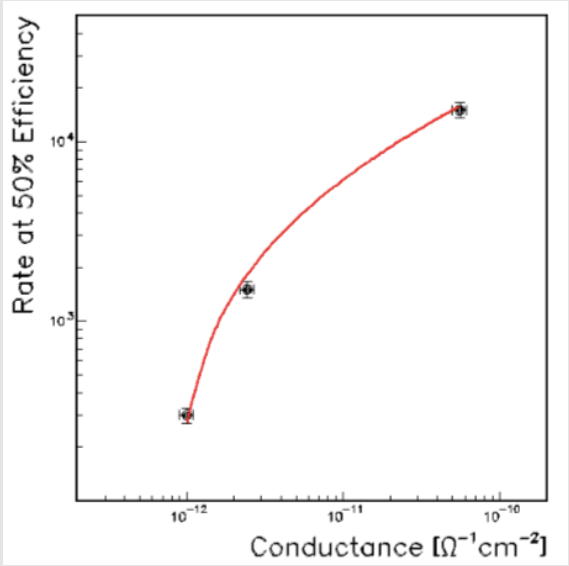

$I_{50\%}=a+bH+cH^3$

where $H = 1/\log_{10}(G)$, where G is the conductance per area of the glass plates; and a, b, and c are free parameters.

$a = 1.7\text{x}10^5$, $b = 3.2\text{x}10^6$ and $c=-1.7\text{x}10^8$.

Secondary Emission Calorimetry

Why Secondary Emission Ionization Calorimeters?

- **Secondary Emission (SE) signal:** Generated with SE surfaces inside electromagnetic/hadronic showers:

  – SE yield δ: Scales with particle momentum

  – SE e^-: $3 < \delta < 100$, per $0.05 < e^- < 100$ keV (material dependent)

  – $\delta \sim 0.05 - 0.1$ SE e^- per MIP

- **SE Calorimetry:** Radiation-Hard + Fast

  – a) Metal-Oxide SE PMT Dynodes survive > 100 GRad

  – b) SE Beam Monitors survive 10^{20} MIPs/cm^2

Expect ~ 60-240 SE e^- per 100 GeV pion shower w/ MIPs alone

BUT in an SE calorimeter module, SE e^- will be amplified exactly like photoelectrons in the PMTs.

SE Sensor Options - 1

- **Etched Metal Sheets:** This option is identical to the Hamamatsu dynodes that are ~ 50 cm long in some existing designs. They are already diced from large sheets. The figure shows the picture of a multi-anode PMT of 5" edge size (left), and sketches of the electron multiplication (middle) and utilization as an SE module with the traversing particle shown with an arrow.

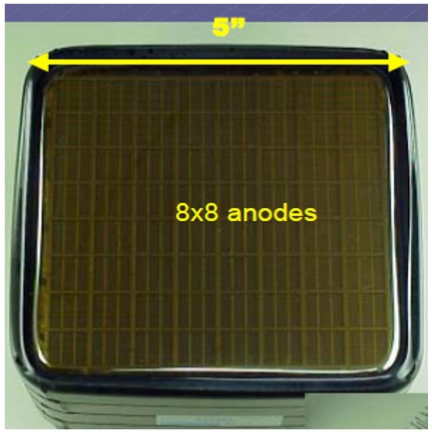

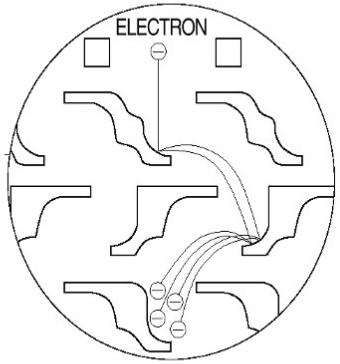

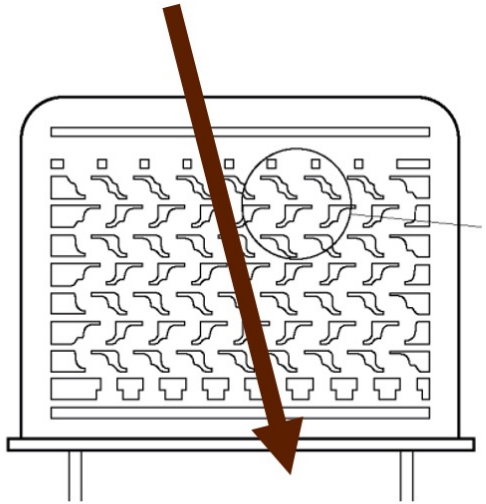

SE Sensor Options - 2

- **Metal Screen Dynodes:** These are basically mesh dynode variants. Usually the dynode separation is 0.9 mm and the wire diameter is 5 μm. The gains of these devices are at the order of 10^5. The figure shows a picture of a similar device and the fine mesh dynode structure.

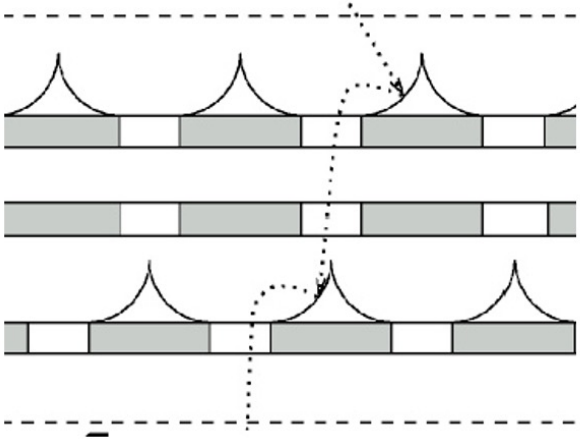

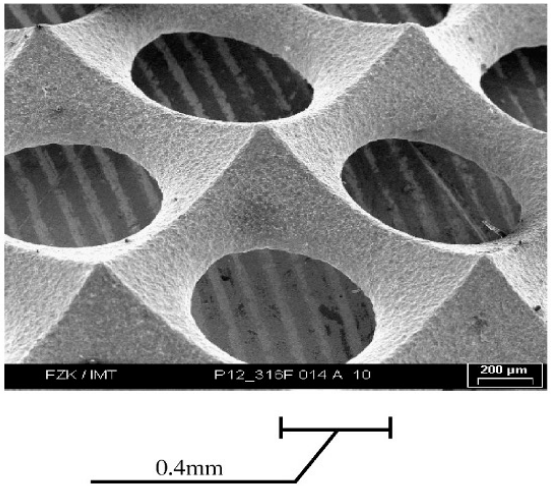

Construction of SE Modules

SE modules with 7 Hamamatsu R7761 19 stage mesh dynode PMTs were constructed. The baseboards were designed to provide three operation modes:

- Normal divider (photomultiplier) mode
- Cathode – first dynode shorted mode
- Floating cathode mode

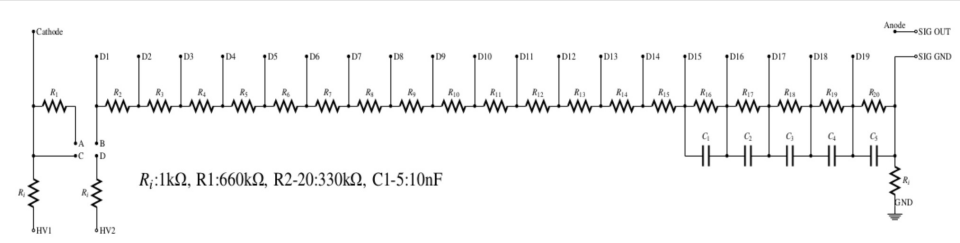

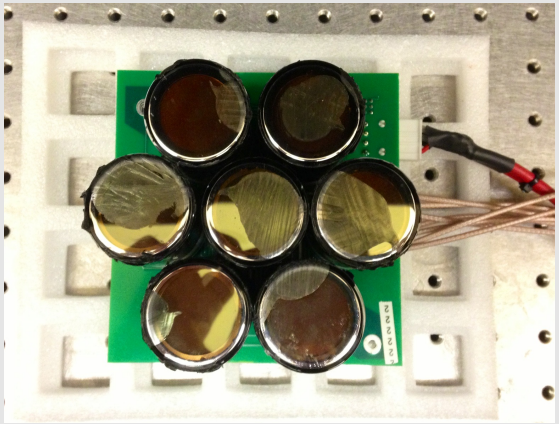

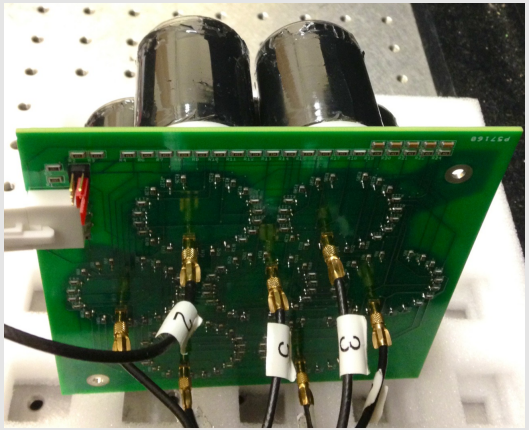

The default operation mode for the SE module was the cathode - first dynode shorted mode (B-C bridge) with an average gain of 6-9×10^5.

E. Tiras, et.al., JINST 11 P10004, 2016

Tests of SE Modules

The SE modules were tested at FTBF with 8 GeV and 16 GeV positrons. The lateral coverage of the modules does not allow an effective measurement of the shower development with steel absorbers. The measurements were taken with the central sensor and up to 16 3 cm × 3 cm × 0.35 cm tungsten absorbers. MC matching is still under development.

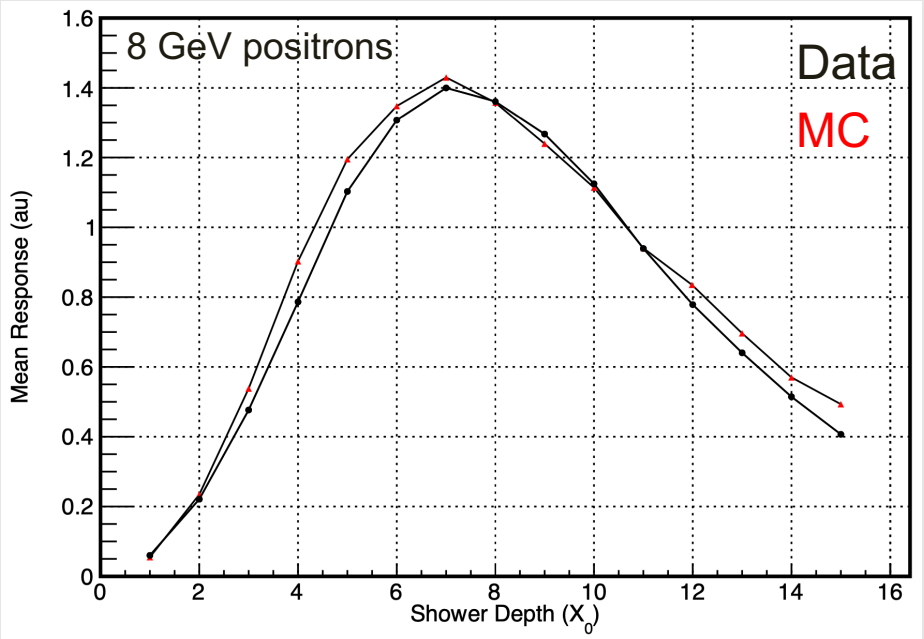

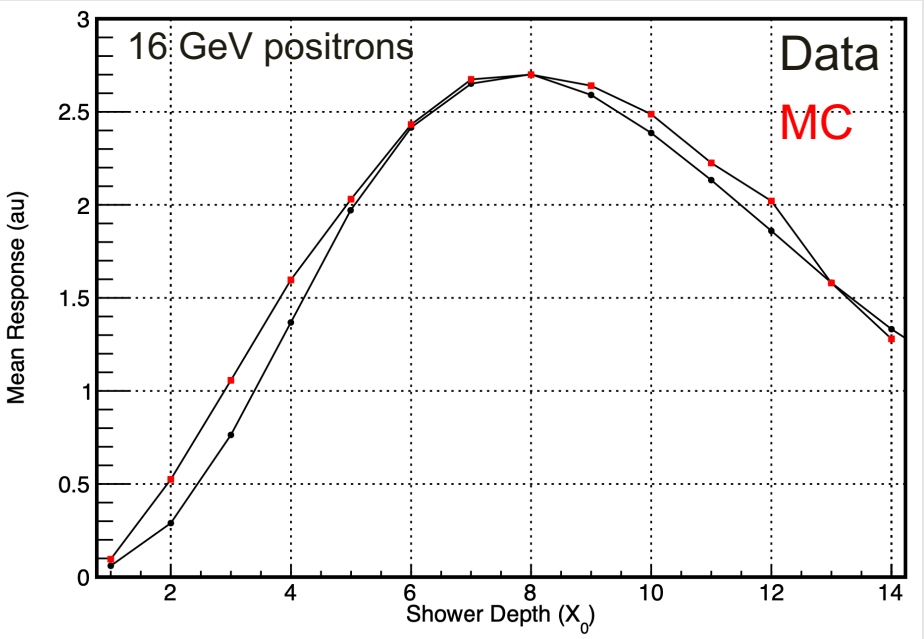

The results validate the principle of SE calorimetry.

Enhancement of Secondary Electron Emission

The cathode and the dynodes of the SE sensors can be made by coating the mesh copper foils with secondary emitters like Al_2O_3, SnO_2, TiO_2 or ZrO_2. The coating can be done with magnetron sputtering with the simplest options being Al_2O_3 and TiO_2.

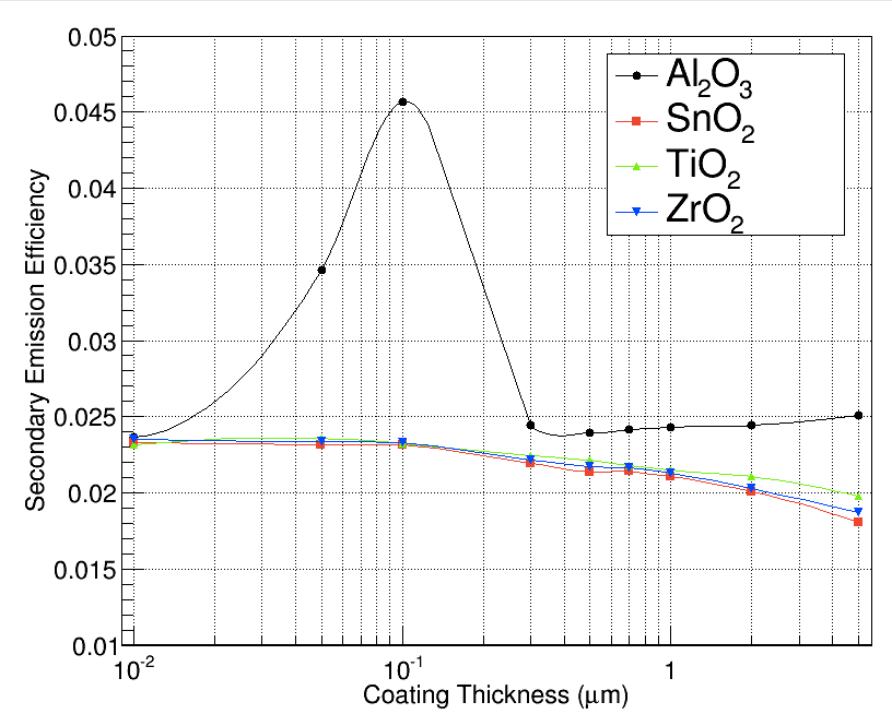

Average secondary electron emission efficiency was calculated for various thicknesses of Al_2O_3, SnO_2, TiO_2 and ZrO_2 with 4 GeV muons (MIP).

The best performance was predicted to be with 100 nm thick Al_2O_3.

Enhancement of Secondary Electron Emission

The secondary electron emission efficiency and the e^- yield of the 100-nm Al_2O_3 coated copper cathode/dynode was simulated as a function of the βγ of the traversing particle (muon). The minimum ionization occurs around βγ of 40 which corresponds to roughly 4 GeV of muon energy. The average secondary electron yield is around 68.

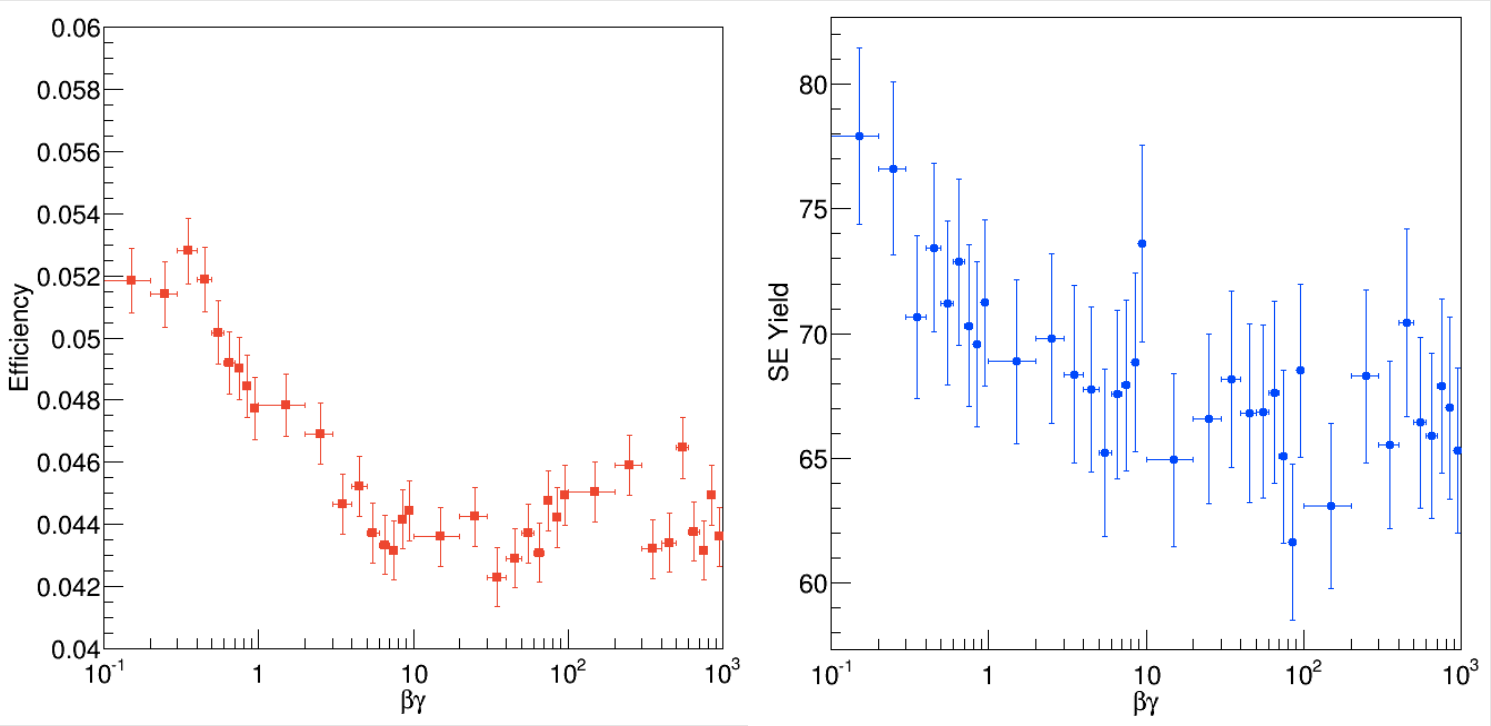

Projection to a Full-Scale SE Sensor

- The mesh structure made by holes of size between 10 and 100 microns and hole spacing of 50 – 100 microns.
- 150 microns distance between the dynode layers.
- Vacuum housing (no dramatic vacuum requirements).
- Start with a 9-stage multiplication.

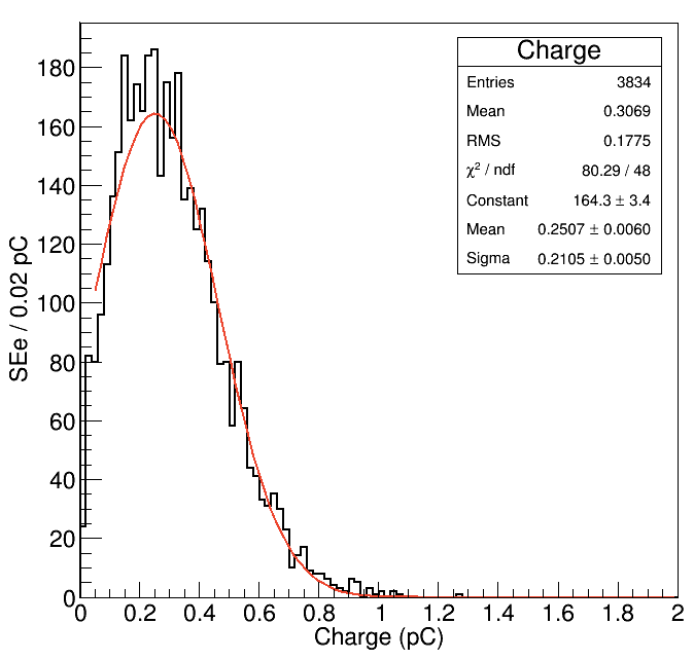

Figure shows the charge spectrum for a 9-stage secondary emission device for a minimum ionizing particle that is efficient at the cathode. With an average of 300 fC, the signal can be recorded with commercial oscilloscopes.

12 and 15 stage SE sensors are also practical.

Projection to a Full-Scale SE Calorimeter

The electromagnetic response of an SE calorimeter prototype with 16 active layers interleaved with 1 X_0 tungsten absorbers is also simulated. The SE sensor is the previously described 9-stage SE device.

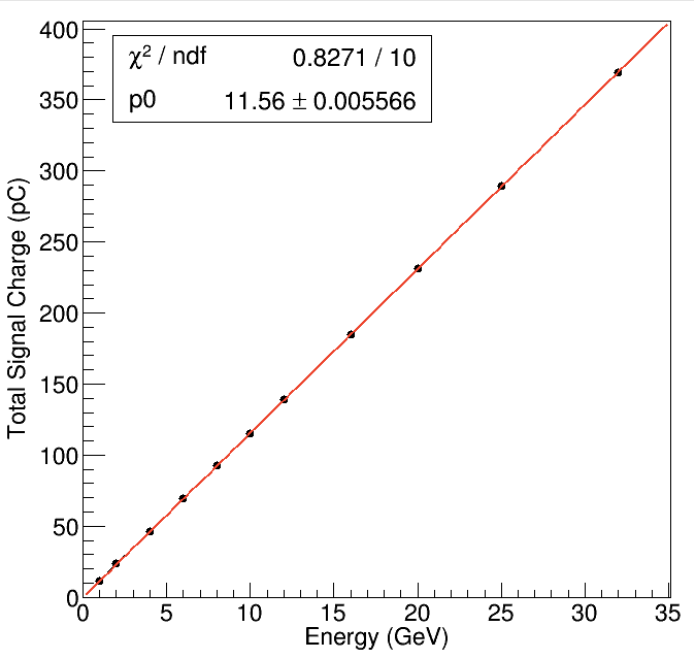

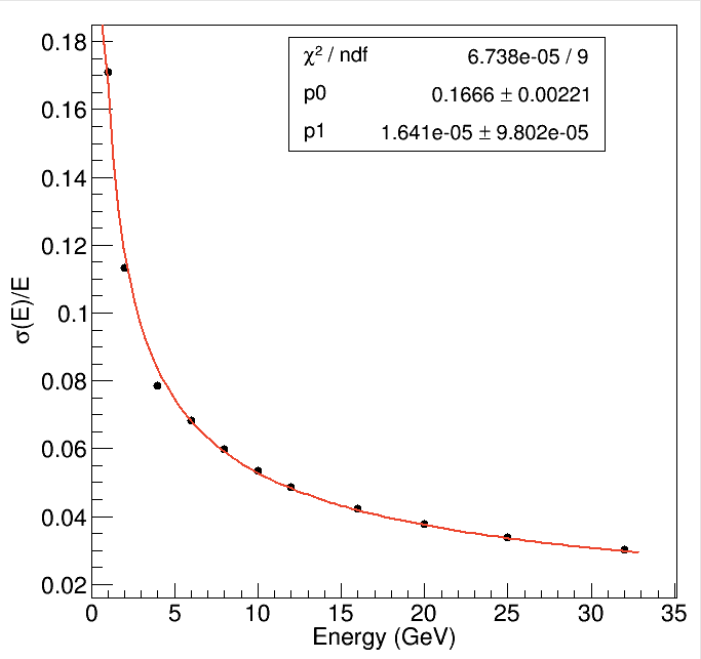

The detector response is linear in the energy range of 1-32 GeV and the electromagnetic energy resolution is obtained as $^{16.7\%}/_{\sqrt{E}}$ with a negligible constant term.

Construction of Dedicated SE Sensors

The construction requirements for an SE Sensor Module are much easier than a PMT, since:

1. The entire final assembly can be done in air. Dynodes used as particle detectors in Mass Spectrometers or in beam monitors cycle to air repeatedly.
2. The thin film deposition procedure and the handling of the coated SE layer are not as delicate procedures as for the photocathodes.
3. The SE module is sealed by normal vacuum techniques.
4. The vacuum necessary is 100 times higher than that needed for a PMT photocathode.

The modules envisioned are compact, high gain, high speed, exceptionally radiation damage resistant, rugged, and cost effective, and can be fabricated in arbitrary tileable shapes. The SE sensor module anodes can be segmented transversely to sizes appropriate to reconstruct electromagnetic cores with high precision.

Conclusions – Digital Hadron Calorimetry

- The first Digital Hadron Calorimeter was built and tested successfully. By construction, the DHCAL was the first large-scale calorimeter prototype with embedded front-end electronics, digital readout, pad readout of RPCs and extremely fine segmentation.

- Fine segmentation allows the study of electromagnetic and hadronic interactions with unprecedented level of spatial detail, and the utilization of various techniques not implemented in the community so far (software compensation, leakage correction, …). The level of detail also introduces challenges in the simulation of the response.

- The novel 1-glass chamber design offers a number of advantages over the traditional two-plate design: an average pad multiplicity close to unity, a reduced overall thickness, a simplified construction procedure and an improvement in rate capability by a factor of 2.

- Raising the overall conductance per unit area of the glass plates will enhance the rate capability and increase the range of particle rates for which the chambers retain their full particle detection efficiency.

- By developing the hybrid RPCs, the heavy requirements on gases are planned to be relaxed by shifting part of the electron multiplication in the gas layer to materials with high secondary electron multiplication capability coated on the anode surface of 1-glass RPCs.

Conclusions – Secondary Emission Calorimetry

- Secondary emission calorimetry is a feasible option particularly for electromagnetic calorimetry in high radiation environments, as well as other implementations such as beam loss monitors and Compton polarimeters.
- The construction of the sensor modules is simple. The envisaged modules are compact, robust and cost effective.
- The preliminary tests validate the idea and suggest a full-scale SE calorimeter prototype.
- Highly segmented readout for imaging calorimetry is possible.

References

- B. Bilki, et.al., Calibration of a digital hadron calorimeter with muons, JINST 3 , P05001, 2008.
- B. Bilki, et.al., Measurement of positron showers with a digital hadron calorimeter, JINST 4, P04006, 2009.
- B. Bilki, et.al., Measurement of the rate capability of Resistive Plate Chambers, JINST 4, P06003, 2009.
- B. Bilki, et.al., Hadron showers in a digital hadron calorimeter, JINST 4, P10008, 2009.
- Q. Zhang, et.al., Environmental dependence of the performance of resistive plate chambers, JINST 5, P02007, 2010.
- J. Repond, Analysis of DHCAL Muon Data, CALICE Analysis Notes, CAN-030, CAN-030A, 2011.
- L. Xia, CALICE DHCAL Noise Analysis, CALICE Analysis Note, CAN-031, 2011.
- B. Bilki, DHCAL Response to Positrons and Pions , CALICE Analysis Note, CAN-032, 2011.
- J. Repond, Analysis of Tungsten-DHCAL Data from the CERN Test Beam, CALICE Analysis Note, CAN-039, 2012.
- B. Bilki, The DHCAL Results from Fermilab Beam Tests: Calibration, CALICE Analysis Note, CAN-042, 2013.
- B. Bilki, et.al., Tests of a novel design of Resistive Plate Chambers, JINST 10, P05003, 2015.
- M. Affatigato, et.al., Measurements of the rate capability of various Resistive Plate Chambers, JINST 10, P10037, 2015.
- N. Johnson, et.al., Electronically Conductive Vanadate Glasses for Resistive Plate Chamber Particle Detectors, International Journal Of Applied Glass Science, 6, 26, 2015.
- B. Freund, et.al., DHCAL with minimal absorber: measurements with positrons, JINST 11, P05008, 2016.
- C. Adams, et.al., Design, construction and commissioning of the Digital Hadron Calorimeter — DHCAL, JINST 11, P07007, 2016.
- M. Chefdeville, et.al., Analysis of testbeam data of the highly granular RPC-steel CALICE digital hadron calorimeter and validation of Geant4 Monte Carlo models, Nucl. Instr. And Meth. A 939, 89, 2019.
- M. Tosun et.al., Development of hybrid resistive plate chambers, Nucl. Instrum. And Meth. A 1054, 168448, 2023.
- E. Tiras et.al., Characterization of photomultiplier tubes in a novel operation mode for Secondary Emission Ionization Calorimetry, JINST 11, P10004, 2016.
- B. Bilki et.al., Secondary Emission Calorimetry, Instruments, 6 48, 2022.